Nuclear Quadrupole Interactions in Copper(II)-Diethylenetriamine-Substituted Imidazole Complexes and in Copper(II) Proteins

Feng Jiang, John McCracken,† and Jack Peisach*

Contribution from the Department of Molecular Pharmacology, Albert Einstein College of Medicine of Yeshiva University, Bronx, New York 10461. *Received May 11, 1990*

Abstract: Electron spin echo envelope modulation spectroscopy was used to study the nuclear quadrupole interactions of the remote ^{14}N of substituted imidazoles coordinated to Cu(II)-diethylenetriamine. Substitution at the carbon adjacent to the remote nitrogen only slightly altered the quadrupole coupling parameters, while alkylation at the remote nitrogen altered them significantly. By applying a modified Townes-Dailey model, we were able to relate the change of quadrupole coupling parameters of the remote nitrogen to the change of electron occupancy in the sp^2 hybrid orbital that is external to the imidazole ring and to relate this to N-H or N-C bond polarization. These studies suggest that the variation of quadrupole coupling constants previously observed in Cu(II) proteins may arise from the variations in hydrogen bonding at the remote nitrogen of the coordinated histidine imidazole side chain.

Electron spin echo envelope modulation (ESEEM) studies have been carried out to identify the metal ligands in various Cu(II) proteins.[1-9] From comparisons with model compounds, it was demonstrated that coordination of histidine imidazole to Cu(II) could be recognized from the nuclear quadrupole interactions (NQI) arising from the remote nitrogen[10] of the coordinated ligand.[11]

Those copper proteins that have been studied thus far fall into two groups. In the first, containing stellacyanin and dopamine β-hydroxylase among others, the NQI parameters for the remote nitrogen of the Cu(II)-coordinated histidine imidazole ligand resemble those obtained for Cu(II)-$(imidazole)_4$ and Cu(II)-(diethylenetriamine)-imidazole model compounds in frozen solution.[2,9,11] In the second group, containing galactose oxidase, amine oxidase, and more specifically phenylalanine hydroxylase, the NQI parameters closely resemble those obtained for Cu(II) model compounds made with 2-methylimidazole rather than with imidazole[4,7b,8] (Figure 1). As the metal ligand in both groups of proteins must undoubtedly be imidazole and not 2-methylimidazole, it was of interest to understand how the NQI parameters of Cu(II)-coordinated imidazole are altered by protein structure.

In order to do so, we carried out ESEEM studies of a series of Cu(II)-diethylenetriamine-substituted imidazole complexes (schematic representation in Figure 2A), where substitutions at different positions of the imidazole ring were used to change the charge distribution on the heterocycle and, in particular, around the remote nitrogen. We also studied the ESEEM of Cu(II)-diethylenetriamine-substituted imidazole complexes in the presence of D_2O and sodium formate, which were shown to alter the local environment near the remote nitrogen. Through the use of spectral simulation, NQI parameters were obtained. It was found that alkyl substitution on the remote nitrogen of imidazole significantly changed NQI parameters, while substitutions on ring carbons or changing of solvent or the introduction of formate had much less effect. By applying the Townes-Daily model,[12] we were able to relate NQI parameters to electron occupancy of the external sp^2 orbital of the remote nitrogen of substituted imidazoles bound to Cu(II). It is suggested from these studies that for Cu(II) proteins having NQI parameters resembling those of Cu(II)-imidazole models, the remote nitrogen of the coordinated histidine ligand is hydrogen bonded to a nucleophile, whereas for those modelled by Cu(II)-2-methylimidazole, the histidine imidazole side chain is more weakly hydrogen bonded or resides in a more hydrophobic environment.

† Present address: Department of Chemistry, Michigan State University, East Lansing, MI 48824.

Table I. Ionization pK_a and Apparent Binding Constant K (mM) of Model Compounds[a]

bases	pK_a (BH^+)	pK[b]
imidazole	6.90	0.307
5-chloro-1-methylimidazole	5.10	-0.656
1-methylimidazole	6.98	0.164
4-methylimidazole	7.35	-0.084
2-methylimidazole	7.77	-0.304
1,2-dimethylimidazole	7.87	-0.326
urocanic acid	5.58	-0.174

[a] Ionization constants were determined by acid-base titration. Apparent binding constants were obtained by optical titration of Cu(II)-dien with each imidazole derivative. [b] The pK is defined as log K.

Experimental Section

Materials. Hydrated cupric acetate was obtained from Mallinkrodt, imidazole from Eastman, and 5-chloro-1-methylimidazole from Frinton Laboratories. 1-Methylimidazole, 2-methylimidazole, 4-methylimidazole, 1,2-dimethylimidazole, 4-imidazoleacetic acid, *N*-acetyl-L-histidine, histamine, urocanic acid, and 4-(hydroxymethyl)imidazole hydrochloride were from Aldrich. Diethylenetriamine was from Fluka AG, and ethylene glycol was from Fisher. Deuterium oxide was from MSD Isotopes. Imidazole and 2-methylimidazole were purified by recrystallization. 4-Methylimidazole was purified by vacuum sublimation. Their purity was verified by melting point. 1-Methylimidazole and 1,2-di-

(1) (a) Mondovi, B.; Graziani, M. T.; Mims, W. B.; Oltzik, R.; Peisach, J. *Biochemistry* **1977**, *16*, 4198-4202. (b) Avigliano, L.; Davis, J. L.; Graziani, M. T.; Marchesini, A.; Mims, W. B.; Mondovi, B.; Peisach, J. *FEBS Lett.* **1981**, *136*, 80-84.
(2) Mims, W. B.; Peisach, J. *J. Biol. Chem.* **1979**, *254*, 4321-4323.
(3) Mims, W. B.; Peisach, J.; Shaw, R. W.; Beinert, H. *J. Biol. Chem.* **1980**, *255*, 6843-6846.
(4) Kosman, D. J.; Peisach, J.; Mims, W. B. *Biochemistry* **1980**, *19*, 1304-1308.
(5) Fee, J. A.; Peisach, J.; Mims, W. B. *J. Biol. Chem.* **1981**, *256*, 1910-1914.
(6) Zweier, J. L.; Peisach, J.; Mims, W. B. *J. Biol. Chem.* **1982**, *257*, 10314-10316.
(7) (a) Mondovi, B.; Morpurgo, L.; Agostinelli, E.; Befani, O.; McCracken, J.; Peisach, J. *Eur. J. Biochem.* **1987**, *168*, 503-507. (b) McCracken, J.; Peisach, J.; Dooley, D. M. *J. Am. Chem. Soc.* **1987**, *109*, 4064-4072.
(8) McCracken, J.; Pember, S.; Benkovic, S. J.; Villafranca, J. J.; Miller, R. J.; Peisach, J. *J. Am. Chem. Soc.* **1988**, *110*, 1069-1074.
(9) McCracken, J.; Desai, P. R.; Papadopoulos, N. J.; Villafranca, J. J.; Peisach, J. *Biochemistry* **1988**, *27*, 4133-4137.
(10) We designate N1 of metal-coordinated imidazole as the remote or amino nitrogen and N3 as the directly coordinated or imino nitrogen, respectively. They are also referred to as the amino nitrogen and the imino nitrogen for noncoordinated imidazole.
(11) Mims, W. B.; Peisach, J. *J. Chem. Phys.* **1978**, *19*, 4921-4930.
(12) Townes, C. H.; Dailey, B. P. *J. Chem. Phys.* **1949**, *17*, 782-796.

0002-7863/90/1512-9035$02.50/0

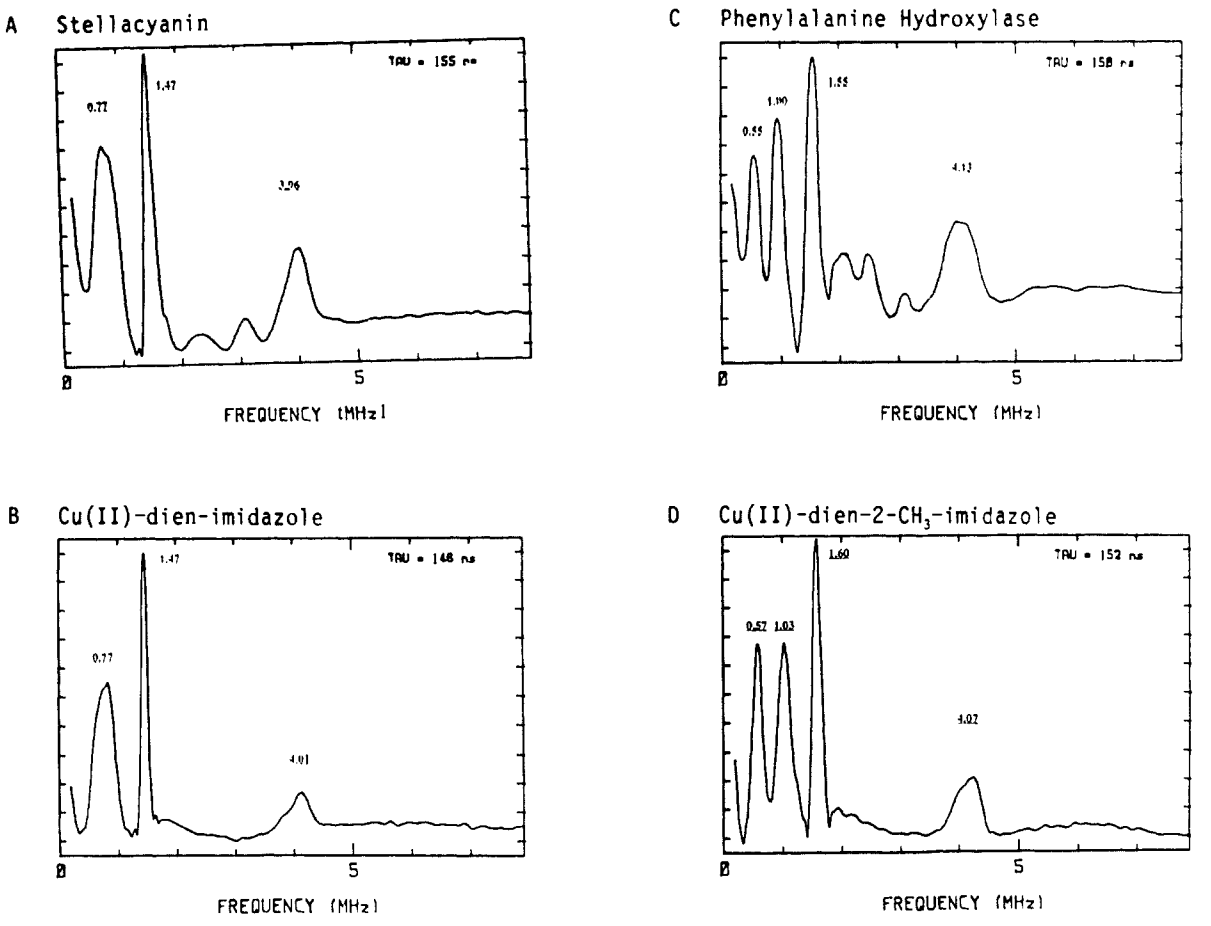

Figure 1. Fourier transformations of ESEEM data for (A) stellacyanin (microwave frequency, 8.854 GHz; magnetic field, 3026 G), (B) Cu(II)–dien–imidazole (microwave frequency, 9.278 GHz; magnetic field, 3220 G), (C) phenylalanine hydroxylase (microwave frequency, 9.023 GHz; magnetic field, 3090 G), and (D) Cu(II)–dien–2-methylimidazole (microwave frequency, 9.025 GHz; magnetic field, 3100 G). Peak positions of lines arising from nuclear quadrupole interactions are indicated in the figure. The spectrum of phenylalanine hydroxylase is reproduced from ref 8.

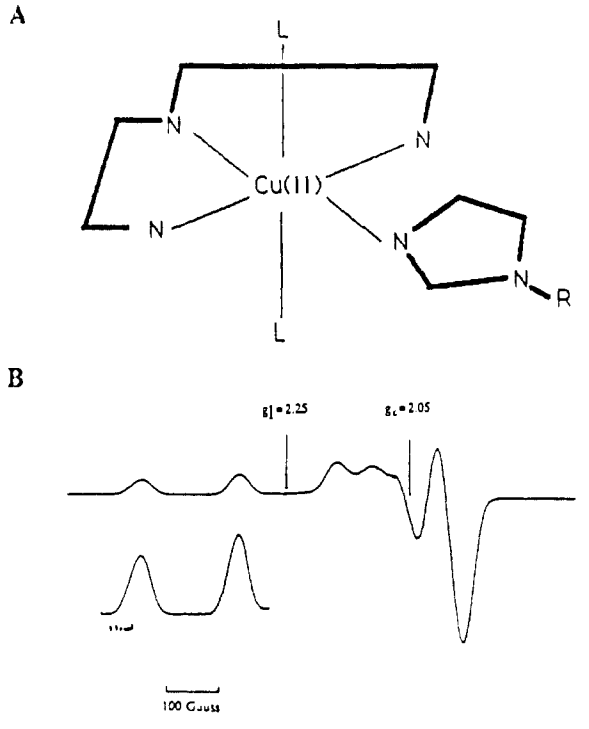

Figure 2. (A) The structure and (B) a typical continuous wave EPR spectrum of Cu(II)–dien coordinated to a substituted imidazole, here 1,2-dimethylimidazole. Measurement conditions: microwave frequency, 9.093 GHz; microwave power, 5 mW; temperature, 77 K; modulation amplitude, 5.0 G; modulation frequency, 100 KHz. The g values are indicated.

methylimidazole, liquid at room temperature, were vacuum distilled, and purity was assessed by density. Deuterated ethylene glycol-$(OD)_2$ was prepared by exchanging the protonated material three times against D_2O and then recovering the product by vacuum distillation. The purity was verified by the refractive index. All other chemicals were used as received. Stellacyanin was prepared as described previously.[2]

pK_a. The pK_a values for substituted imidazoles (Table I), used in the calculation of binding constants of Cu(II)–diethylenetriamine with these compounds, were determined from inflection points in acid–base titration curves obtained with a Radiometer PHM 72 Mk2 digital acid–base analyzer. The pK_a's for imidazole, 2-methylimidazole, 4-methylimidazole, and 1,2-dimethylimidazole are consistent with previous reports.[13]

Binding Constants. The binding constants measured by optical titration are expressed as apparent binding constants. The d^9 ground-state Cu(II) can bind strongly to four ligands in the equatorial plane. Because the sequential and simultaneous association of four equatorial ligands make the quantitative analysis of binding difficult, diethylenetriamine (dien), a tridentate ligand for Cu(II), was used to occupy three of the equatorial binding sites. Then, Cu(II)–dien was titrated with a substituted imidazole.

Cu(II)–dien was prepared in aqueous solution by using 2 mM Cu(II) with 2.4 mM dien. The pH was adjusted to 7.5. The complex thus formed was characterized optically (ϵ_{609} = 87.6 cm^{-1} M^{-1}). Small volume increments of 1 M substituted imidazole, pH adjusted to 7.5 with acetic acid, were then added. After each addition, the pH was readjusted to 7.5 with concentrated sodium hydroxide. A Cary 14 spectrophotometer, converted to microprocessor control by Aviv Associates, was used to record the absorption spectrum. Isosbesticity was retained throughout each titration. Apparent binding constants were obtained by computer aided, iterated least-square fit of the data.[14] In the analysis, the con-

(13) Walker, F. A.; Lo, M. W.; Ree, M. T. *J. Am. Chem. Soc.* **1976**, *98*, 5552–5560.
(14) Park, C. M.; Nagel, R. L.; Blumberg, W. E.; Peisach, J.; Magliozzo, R. S. *J. Biol. Chem.* **1986**, *261*, 8805–8810.

centration of Cu(II) was the fixed parameter, and the total concentration of added ligand and the optical absorbance were input data. The pK_a values for substituted imidazoles were used to correct for the concentration of deprotonated, free ligand. Results are given in Table I.

Sample Preparations. Complexes used for ESEEM studies were prepared with 2.0 mM cupric acetate, 2.4 mM dien, and substituted imidazoles at those concentrations where at least 95% of the optical spectral change was obtained in a titration. The pH of each sample was 7.5. Ethylene glycol (1:1, v:v) was included to assure good glass formation, a requisite for magnetic resonance investigations of frozen solution samples. For samples in D_2O, complexes were prepared in the same way as in H_2O, but with deuterated ethylene glycol. For the formate-containing samples, excess solid sodium formate was added to saturation to a solution of Cu(II)–dien-substituted imidazole, before ethylene glycol was added. The final concentration of sodium formate in the sample was 5–6 M.

Spectroscopy and Spectral Simulations. Continuous wave (CW) X-band EPR spectra were obtained with a Varian E112 spectrometer. The spectrum for each complex studied confirmed its paramagnetic purity, in accord with results obtained by optical titration. All the Cu(II)–dien-substituted imidazole complexes studied had typical axial **g** and **A** tensors (Figure 2B). On the basis of spectral simulation,[15] $\mathbf{g}_\perp = 2.050$, $\mathbf{g}_\parallel = 2.215$, $A_\perp = 70.0$ MHz, and $A_\parallel = 580.0$ MHz, for the Cu(II)–dien–1,2-dimethylimidazole complex. The spectra for all the other imidazole derivatives and those in the presence of sodium formate or D_2O had the same **g** and **A** values, except that the relative intensities of $\mathbf{g}_\parallel$ and $\mathbf{g}_\perp$ features were slightly different.

ESEEM experiments were performed on a home-built pulsed EPR spectrometer,[7b] with a folded strip-line cavity,[16] by using the stimulated echo ($90°$–τ–$90°$–T–$90°$) pulse sequence. The τ values used to collect the data shown here were set to periods of proton Zeeman frequency harmonics so that modulations due to weakly coupled protons were largely suppressed.[17a] Typical measurement conditions were the following: microwave frequency, 8.8 GHz; magnetic field strength, 3100 G; microwave power, 45 W; pulse width, 20 ns; sample temperature, 4.2 K; pulse repetition rate, 100 Hz. Fourier transformations using a method described previously[9] gave the ESEEM spectra.

ESEEM arises from weak magnetic coupling between Cu(II) and neighboring nuclei. For square-planar Cu(II)–dien-substituted imidazole complexes, the coupling of directly coordinated, equatorially bound ^{14}N is too large to give rise to envelope modulation.[11] Only the superhyperfine coupling between Cu(II) and the remote ^{14}N of coordinated imidazole contributes to the ESEEM.

The spin Hamiltonian for ^{14}N is given by

$$\mathcal{H}_N = -g_N\beta_N\mathbf{HI} + \mathbf{SA}_N\mathbf{I} + \hbar\mathbf{IQI} \qquad (1)$$

The first term is the nuclear Zeeman interaction, where g_N and β_N are nuclear g factor and Bohr magneton, **H** is the external magnetic field, and **I** is the nuclear spin operator. The second term is the electron-nuclear superhyperfine interaction, where $\mathbf{A}_N$ is the superhyperfine tensor and **S** is the electron spin operator. The third term is the nuclear quadrupole interaction, where $\hbar$ is Planck's constant and **Q** is the quadrupole interaction tensor.

At X-band, the nuclear Zeeman term, $g_N\beta_N\mathbf{H}$, for the remote nitrogen (N1) of Cu(II)-coordinated imidazole is approximately equal to one-half its electron-nuclear coupling term, **AI**·**S**,[11] characteristic of the "exact cancellation condition".[18] Therefore, for one of the ^{14}N spin manifolds, the two terms almost cancel, leaving the nuclear quadrupole interaction to solely determine the energy level splitting (Figure 3A). This gives rise to three sharp lines in the ESEEM spectrum, where the frequencies of two add to give the third (Figure 3B). The other spin manifold, where the nuclear Zeeman term is doubled by the electron-nuclear coupling, gives a single broad line at about four times the nuclear Zeeman frequency, encompassing a $\Delta M_I = 2$ transition. The two $\Delta M_I = 1$ transitions from the second manifold are highly orientation dependent[19] and are not resolved in powder samples.

Simulation of ESEEM spectra was carried out by using the density matrix formalism of Mims,[20] together with the angle-selected averaging

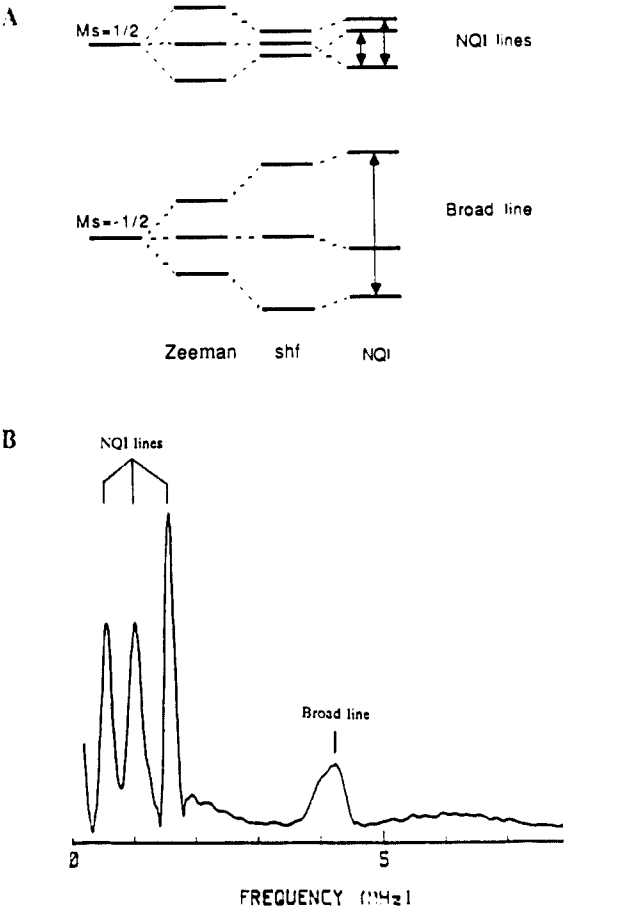

Figure 3. (A) Electron spin energy level scheme for ^{14}N and (B) Fourier transformation of ESEEM obtained at the condition of near cancellation of nuclear Zeeman and hyperfine terms of the spin Hamiltonian for ^{14}N. The three NQI lines are designated ν_0, ν_+, ν_-.

scheme developed by Hurst et al.[21] for interpretation of ENDOR shifts from randomly oriented transition-metal complexes. The NQI parameters, including the quadrupole coupling constant e^2qQ and the asymmetry parameter η, measure the magnitude and the symmetry of the efg tensor.

$$e^2qQ = e^2q_{zz}Q \qquad (2)$$

$$\eta = (q_{xx} - q_{yy})/q_{zz} \qquad (3)$$

Here q_{ii} ($i = x, y, z$) are the principal values of the **efg** tensor[22] and Q is the nuclear quadrupole moment. As long as the conditions for exact cancellation are approximately satisfied ($\mathbf{A}_{iso}/2 \simeq g_N\beta_N\mathbf{H}$), the NQI parameters can be determined from the frequencies (eqs 4 and 5) of three sharp "zero field" nuclear quadrupole resonance lines[11] in the ESEEM spectrum.

$$\nu_\pm = {}^3/_4e^2qQ(1 \pm \eta/3) \qquad (4)$$

$$\nu_0 = {}^1/_2e^2qQ\eta \qquad (5)$$

The relative orientation of the principal axis of the **efg** tensor to that of the **g** tensor changes the relative intensities of these lines, and, together with $\mathbf{A}_{iso}$, the electron-nuclear coupling parameters and r, the effective distance between the unpaired electron and its interacting nucleus, determines the shape and frequency of the broad, high frequency line.[23] Because of the uncertainty of the relative orientation of two principal axis

(15) (a) Nilges, M. J. Ph.D. Thesis, University of Illinois, Urbana, IL, 1979. (b) Belford, R. L.; Nilges, M. J. *International Electron Paramagnetic Resonance Symposium*; 21st Rocky Mountain Conference, Denver, CO, 1979. (c) Maurice, A. M. Ph.D. Thesis, University of Illinois, Urbana, IL, 1981.
(16) Britt, R. D.; Klein, M. P. *J. Magn. Reson.* **1987**, *74*, 535–540.
(17) (a) Mims, W. B.; Peisach, J. *Biological Magnetic Resonance*; Berliner, L. J., Reuben, J., Eds.; Plenum Press: New York, 1981; Vol. 3, pp 213–263. (b) Kevan, L. *Time Domain Electron Spin Resonance*; Kevan, L., Schwartz, R. N., Eds.; Wiley-Interscience: New York, 1979; pp 279–342.
(18) Flanagan, K. L.; Singel, D. J. *J. Chem. Phys.* **1987**, 5606–5616.
(19) Colaneri, M.; Peisach, J. *J. Am. Chem. Soc.* In press.
(20) Mims, W. B. *Phys. Rev.* **1972**, *5*, 2409–2419.
(21) (a) Hurst, G. C.; Henderson, T. A.; Kreilick, R. W. *J. Am. Chem. Soc.* **1985**, *107*, 7294–7299. (b) Henderson, T. A.; Hurst, G. C.; Kreilick, R. W. *J. Am. Chem. Soc.* **1985**, *107*, 7299–7303.
(22) Lucken, E. A. C. *Nuclear Quadrupole Coupling Constants*; Academic Press: New York, 1969; pp 217–248.
(23) (a) McCracken, J.; Cornelius, J. B.; Peisach, J. *Pulsed EPR: A New field of Applications*; Keijzers, C. P., Reijerse, E. J., Schmidt, J., Eds.; North Holland Publ.: Amsterdam, 1989; pp 156–161. (b) Cornelius, J. B.; McCracken, J.; Clarkson, R.; Belford, R. L.; Peisach, J. *J. Phys. Chem.* **1990**, *94*, 6977–6982.

Table II. NQI Frequencies Obtained by Fourier Transformation of ESEEM Data, Superhyperfine Coupling Parameters, and Differences of Electron Occupancy ($c - c_0$) at the N-H or N-R σ Bond of the Remote Nitrogen of Cu(II)-Dien-Substituted Imidazole Complexes

	ligands	ν_0	ν_+	ν_-	A_{iso} (MHz)	r (Å)	e^2qQ (MHz)	η	$c - c_0$	$\Delta(c - c_0)^a$
1[b]	imidazole	0.65	0.83	1.47	1.55	2.90	1.43	0.94	0.185	0.025
2	4-imidazoleacetic acid	0.67	0.87	1.51	1.51	2.75	1.46	0.94	0.183	0.002
3	4-(hydroxymethyl)imidazole	0.68	0.87	1.49	1.45	2.75	1.43	0.96	0.182	0.022
4	*N*-acetyl-L-histidine	0.70	0.92	1.52	1.39	2.75	1.47	0.96	0.171	0.000
5	4-(2-piperidylethyl)imidazole	0.70	0.83	1.56	1.47	2.90	1.54	0.98	0.168	0.044
6	urocanic acid	0.81	0.81	1.56	1.40	2.90	1.52	0.98	0.169	0.020
7	4-methylimidazole	0.59	0.96	1.55	1.54	3.00	1.60	0.75	0.143	0.010
8	2-methylimidazole	0.57	1.03	1.60	1.80	3.25	1.73	0.64	0.122	0.000
9	2-ethylimidazole	0.57	1.03	1.60	1.83	3.25	1.73	0.64	0.122	0.000
10	5-chloro-1-methylimidazole	0.27	1.59	1.91	1.61	3.75	2.31	0.28	0.023	0.109
11	1-methylimidazole	0.15	1.46	1.65	1.92	3.50	2.06	0.20	0.042	0.044
12	1-benzylimidazole	0.17	1.46	1.65	1.88	3.25	2.06	0.20	0.042	0.044
13	1,2-dimethylimidazole	0.17	1.66	1.84	2.20	4.10	2.33	0.11	0.000	0.000

[a] The uncertainty of $c - c_0$ in fitting the data to calculated values. [b] The numbers preceding the name of each model compound are referred to in Figures 7 and 8. Compounds 1–6 are designated group 1, 7–9, group 2, and 10–13, group 3.

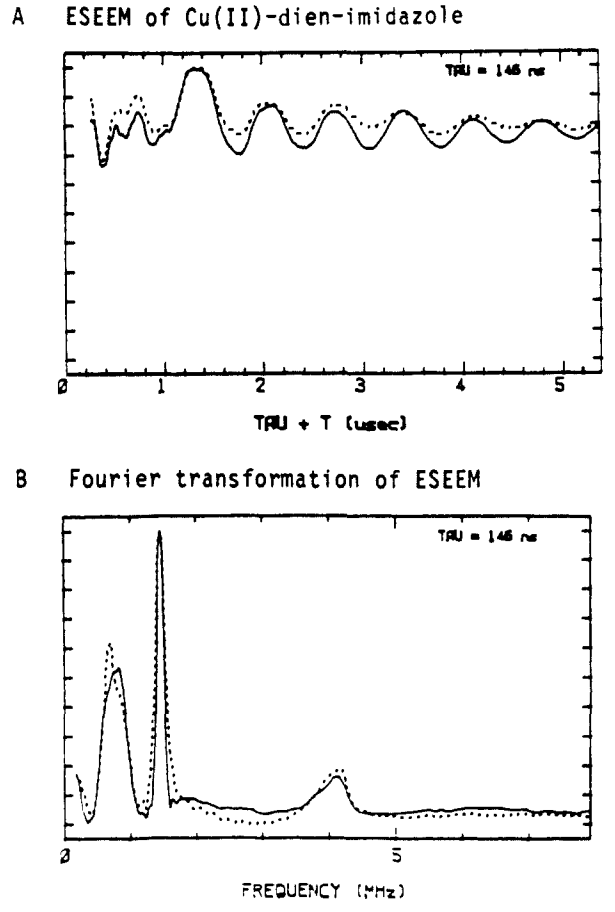

Figure 4. (A) ESEEM data and (B) Fourier transformation for Cu(II)-dien-imidazole. Measurement conditions are as follows: microwave frequency, 9.276 GHz; magnetic field, 3220 G; sample temperature, 4.2 K. Simulation parameters are as follows: A_{iso}, 1.55 MHz; r, 2.90 Å; e^2qQ, 1.43 MHz; η, 0.94. Solid lines, experimental data; dashed lines, simulation.

systems (PAS),[24] the simulations were carried out assuming the same Euler angles between two PAS's (0°, 0°, 0°) and the same $\theta_N\phi_N$ (90°, 0°) angles which describe the relative orientation of the remote nitrogen (N1) to the PAS of the **g** tensor.

Figure 4A gives the ESEEM experimental data and the simulation for Cu(II)-dien-imidazole, and Figure 4B gives the Fourier transformations. The values of e^2qQ and η obtained this way, 1.43 and 0.94, are consistent with values obtained by a NQR study of solid-state imidazole, 1.424 ± 0.001 and 0.98 ± 0.07.[25] Since our prime interest here is the NQI parameters, the uncertainty of the relative orientations of the PAS does not affect our results and subsequent conclusions.

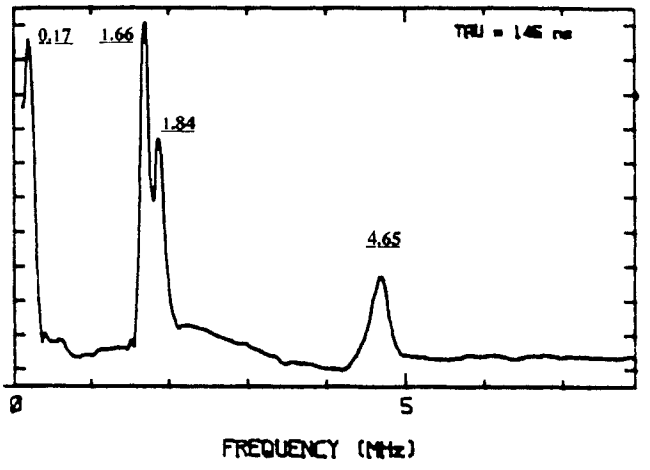

Figure 5. Fourier transformation of ESEEM for Cu(II)-dien-1,2-dimethylimidazole. Measurement conditions are as follows: microwave frequency, 9.300 GHz and magnetic field, 3230 G.

Results

For the remote or the amino nitrogen of Cu(II)-coordinated substituted imidazole, the NQI parameters obtained by ESEEM simulation fall into three groups (Table II). Typical spectra are shown in Figures 1 and 5. The first group, compounds 1–6, consists of imidazole and those derivatives having C4 substituted with electron-withdrawing groups. They have an asymmetry parameter, η, close to 1, characterized by two poorly resolved, low-frequency NQI lines and one well-separated high-frequency line (Figure 1B). The second group, compounds 7–9, includes 2-methyl-, 2-ethyl-, and 4-methylimidazole, where the carbon next to the remote nitrogen is substituted with an alkyl group. These compounds have smaller asymmetry parameters and give three, well-resolved, sharp NQI lines in the ESEEM spectrum, indicative of a decrease of η away from unity (Figure 1D). For the last group, compounds 10–13, where the proton at the remote nitrogen of imidazole is substituted by an alkyl group, the largest perturbation of the **efg** is observed, η is decreased to near zero, and the two lower NQI lines separate more, so that the middle line nearly coalesces with the upper line (~0.2-MHz separation) (Figure 5).

Discussion

Electron Orbital Occupancy at the Remote Nitrogen. The NQI is defined as the interaction between the nuclear quadrupole moment and the electric field gradient generated by electrons and

(24) The ring plane of imidazole in frozen solution orientates randomly. The PAS of the **efg** tensor at the remote nitrogen is fixed relative to the imidazole ring plane. Therefore, the uncertainty of the orientation of the imidazole ring plane with respect to the PAS of the **g** tensor causes the uncertainty of the PAS of the **efg** of the remote nitrogen in relation to the PAS of the **g** tensor.

(25) Hunt, M. J.; Mackay, A. L.; Edmonds, D. T. *Chem. Phys. Lett.* **1975**, *34*, 473–475.

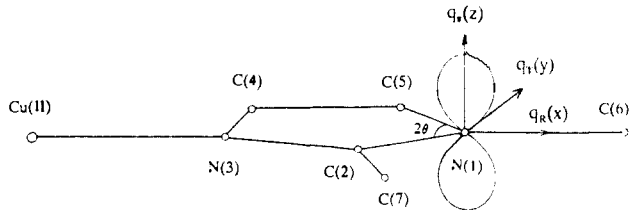

Figure 6. The orientation of the electric field gradient axis system at the remote nitrogen (N(1)) of Cu(II)-coordinated 1,2-dimethylimidazole. ϕ_s, ϕ_x, ϕ_y, and ϕ_z are wave functions of $2p_s$, $2p_x$, $2p_y$, and $2p_z$ atomic orbitals. ψ_1, ψ_2, ψ_3, and ψ_4 are wave functions of the nitrogen atomic orbitals along the N(1)–C(6) bond, the N(1)–C(5) bond, the N(1)–C(2) bond, and the z axis, respectively. a, b, b, and c are the corresponding electron orbital occupancies.

ions around that nucleus. According to the Townes–Dailey model,[12] the change of the electric field gradient at a quadrupolar nucleus, such as ^{14}N, is attributed mainly to electrons in the valence shell p orbitals of that atom. For Cu(II)–dien–imidazole, substitutions at different positions of the heterocycle ring produce a change of the electron distribution in the molecular orbitals of imidazole and, therefore, a change of the electron occupancy in the valence shell orbitals of the remote nitrogen, leading to a change in the electric field gradient. In other words, the change of NQI parameters caused by ring substitution is due to a change of electron occupancy in the valence shell p orbitals of the remote nitrogen. To understand how ring substitution causes this change, comparison is made with a reference compound, Cu(II)–dien–1,2-dimethylimidazole, which has the lowest asymmetry parameter and, as will be shown in the text below, the lowest electron orbital occupancy in the external sp^2 hybrid orbital of all the model compounds studied here.

For the remote nitrogen of Cu(II)–dien–1,2-dimethylimidazole (Figure 6), the valence shell has three nontrigonal sp^2 hybrid orbitals and one p orbital. The wave functions are given by

$$\psi_1 = \cot\theta\phi_s + (1 - \cot^2\theta)^{1/2}\phi_x \quad (6)$$

$$\psi_2 = 1/\sqrt{2}(1 - \cot^2\theta)^{1/2}\phi_s - 1/\sqrt{2}\cot\theta\phi_x + 1/\sqrt{2}\phi_y \quad (7)$$

$$\psi_3 = 1/\sqrt{2}(1 - \cot^2\theta)^{1/2}\phi_s - 1/\sqrt{2}\cot\theta\phi_x - 1/\sqrt{2}\phi_y \quad (8)$$

$$\psi_4 = \phi_z \quad (9)$$

Here it is assumed that the z axis is perpendicular to the imidazole plane and the x axis coincides with the sp^2 hybrid orbital that is external to the heterocyclic ring.

If we assume that the two N–C sp^2 orbitals at the remote nitrogen have approximately equal electron occupancies[26] and that b is the electron occupancy of each of them, a is that of the $p\pi$ orbital, c is that of the external N–H or N–R (for N-alkylated imidazoles) sp^2 orbital, and θ is half the remote nitrogen CNC bond angle, then the **efg** tensor can be written as[28]

$$q_\pi = q_0[a - 1/2(1 + \cot^2\theta)b - 1/2(1 - \cot^2\theta)c] \quad (10)$$

$$q_R = q_0[-a/2 + (\cot^2\theta - 1/2)\,b + (1 - \cot^2\theta)c] \quad (11)$$

$$q_T = q_0[-a/2 + (1 - 1/2\cot^2\theta)b - 1/2(1 - \cot^2\theta)c] \quad (12)$$

For the remote nitrogen of 1,2-dimethylimidazole, each of the three sp^2 hybridized orbitals contains one valence electron from ^{14}N. Two form σ bonds with ring carbons, while the third forms a σ bond with the external carbon of the methyl substituent. The p_z orbital of the remote nitrogen is partially incorporated into the aromatic π system and the two remaining electrons partially delocalize to orbitals of other atoms. Substitution of the N–CH_3 by N–H leads to a change of electron occupancy of the external sp^2 orbital, which then induces changes in the p and the other two sp^2 orbitals as well. Substitution on an imidazole ring carbon induces a change of electron occupancy of the $p\pi$ orbital of the remote nitrogen, which then induces changes of the other three sp^2 orbitals.

If we assume a linear relationship between the electron occupancy of different orbitals and follow $c - c_0$, the change of the electron occupancy at the external sp^2 orbital of each substituted imidazole relative to 1,2-dimethylimidazole, we can express the electron occupancy at other orbitals by the linear relationships

$$a = a_0 - A(c - c_0) \quad (13)$$

$$b = b_0 - B(c - c_0) \quad (14)$$

Here, a_0, b_0, and c_0 refer to electron occupancies of the nitrogen $p\pi$, ring sp^2, and external sp^2 orbitals, respectively, of the reference compound 1,2-dimethylimidazole, while a, b, and c refer to those of any model compound. A and B are proportionality constants which measure the magnitude of the inductive effect (see below).

Since the remote nitrogen of all the imidazole derivatives has the same electron configuration, eqs 10, 11, and 12 are valid for all of them. By replacing a and b in eqs 10, 11, and 12 with eqs 13 and 14, we obtain the three principal values of the **efg** tensor, q_π, q_R, q_T, as functions of $c - c_0$, as follows

$$q_\pi = q_{\pi 0} + q_0[A - 1/2(1 + \cot^2\theta)B - 1/2(1 - \cot^2\theta)](c - c_0) \quad (15)$$

$$q_R = q_{R0} + q_0[-A/2 + (\cot^2\theta - 1/2)B + (1 - \cot^2\theta)](c - c_0) \quad (16)$$

$$q_T = q_{T0} + q_0[-A/2 + (1 - 1/2\cot^2\theta)B - 1/2(1 - \cot^2\theta)](c - c_0) \quad (17)$$

Here $q_{\pi 0}$, q_{R0}, and q_{T0} are the three principal values of the **efg** tensor for the reference compound, 1,2-dimethylimidazole.

The p character and the highest electron occupancy of the $p\pi$ orbital allows us to assume that the largest **efg** tensor, designated z, lies along the p orbital, perpendicular to the ring plane (Figure 6).[29] This is supported by a single-crystal ESEEM study[19] of Cu(II)-doped Zn(II)(1,2-dimethylimidazole)$_2$Cl$_2$, where it was also shown that the x axis is aligned approximately along the methyl C–N bond, within the ring plane. Therefore, for 1,2-dimethylimidazole, $q_{\pi 0} = q_{zz0}$, $q_{R0} = q_{xx0}$, and $q_{T0} = q_{yy0}$.

For the axis system chosen, we obtain a relationship between the NQI parameters and the electron orbital occupancy of the N–R or N–H sp^2 orbital for other substituted imidazoles in terms of the electron orbital occupancy of the reference compound, 1,2-dimethylimidazole, as follows:

$$e^2qQ = \{[a_0 + A(c - c_0)] - 1/2(1 + \cot^2\theta) \times [b_0 + B(c - c_0)] - 1/2(1 - \cot^2\theta)c\}e^2q_0Q \quad (18)$$

$$\eta = 3/2(1 - \cot^2\theta)\{c - [b_0 + B(c - c_0)]\} \quad (19)$$

Proportionality Constants. As argued previously in analogous NQR studies of metal-coordinated pyridine and imidazole complexes,[27,30,31] constraints are placed on the values of A and B. First, the increase of electron occupancy at the external sp^2 orbital caused by replacing an alkyl group with the less electronegative hydrogen

(26) In an early NQR study of metal-coordinated imidazoles, Ashby et al.[27a] applied the modified Townes–Dailey model to interpret their NQR results for the directly coordinated nitrogen. They assumed that one principal axis was directed along the CNC angle bisector with two N–C bonds having equal electron populations, even though the principal axis of the imino nitrogen was shown to be 4° off the CNC bisector. We will use the same assumption for the amino (remote) nitrogen of Cu(II)–dien coordinated imidazoles.

(27) (a) Ashby, C. I. H.; Cheng, C. P.; Brown, T. L. *J. Am. Chem. Soc.* **1978**, *100*, 6057–6063. (b) Ashby, C. I. H.; Cheng, C. P.; Duesler, E. N.; Brown, T. L. *J. Am. Chem. Soc.* **1978**, *100*, 6063–6067. (c) Ashby, C. I. H.; Paton, W. F.; Brown, T. L. *J. Am. Chem. Soc.* **1980**, *102*, 2990–2998.

(28) We use the terminology radial (R), tangential (T), and (π) for direction; R lies close to the internal bisector of the CNC angle, T is close to tangential to the ring apex, and π is along the $p\pi$ orbital of nitrogen, which is perpendicular to the ring. In a later simulation,[22,27] e^2q_0Q/h, the coupling constant generated by an electron in a valence 2p orbital of ^{14}N is 9.0 MHz.

(29) The normal NQR convention for the PAS of the **efg** tensor is $|q_{zz}| > |q_{yy}| > |q_{xx}|$.

(30) Hsieh, Y. N.; Rubenacker, G. V.; Cheng, C. P.; Brown, T. L. *J. Am. Chem. Soc.* **1977**, *99*, 1384–1389.

(31) Rubenacker, G. V.; Brown, T. L. *Inorg. Chem.* **1980**, *19*, 392–398.

Table III. NQI Frequencies Obtained by Fourier Transformation of ESEEM Data, ^{14}N Quadrupole Coupling Constants, and Differences of Electron Occupancy ($c - c_0$) at the N–H σ Bond of the Remote Nitrogen of Histidine Side Chains in Various Copper Proteins

	protein	ν_0	ν_+	ν_-	e^2qQ (MHz)	η	$c - c_0$	$\Delta(c - c_0)^a$	ref
14[b]	dopamine β-hydroxylase[c]	0.7	0.7	1.4	1.44	0.98	0.179	0.010	9
15	stellacyanin[c]	0.77	0.77	1.47	1.49	0.94	0.168	0.001	this work
16	conalbumin[d]	0.7	0.8	1.5	1.53	0.91	0.162	0.001	6
17	laccase[d]	0.59	0.80	1.48	1.52	0.89	0.162	0.003	1a
18	ascorbate oxidase[d]	0.61	0.89	1.54	1.56	0.83	0.153	0.003	1b
19	galactose oxidase[d]	0.55	1.0	1.53	1.70	0.65	0.125[e]	0.002	4
20	phenylalanine hydroxylase[c]	0.55	1.00	1.55	1.68	0.55	0.118[e]	0.078	8
							0.394[f]	0.000	
21	amine oxidase[d]	0.45	1.1	1.55	1.73	0.48	0.106[e]	0.087	7b
							0.387[f]	0.027	

[a] The uncertainty of $c - c_0$ in fitting the data to calculated values. [b] The numbers preceding the name of each protein are used in Figures 7 and 8. [c] The published ^{14}N quadrupole coupling constants were obtained by spectral simulation. [d] The ^{14}N quadrupole coupling constants were calculated from three NQI frequencies of published ESEEM spectra. [e] δ was minimized at $0 < c - c_0 < 0.304$. [f] δ was minimized at $0 < c - c_0 < 1$.

should be compensated for by a decrease of electron occupancy at the other three orbitals. That is, a and b become less than a_0 and b_0 when c becomes greater than c_0. Therefore, A and B must be positive. Second, the total inductive decrease of the electron orbital occupancy in the other three orbitals caused by ring substitution should be no more than the increase of the electron orbital occupancy in the N–H sp^2 orbital. This increase cannot be greater than unity, the difference in occupancy between deprotonated and protonated nitrogen. Therefore, $A + 2B$ should be less than unity. Combining these two constraints, we have

$$0 < A + 2B < 1 \tag{20}$$

If we assume that there is no change in the geometry around the remote nitrogen upon substitution on the imidazole ring, the relationship of A, B, and θ should hold for all the substituted imidazoles studied. By eliminating c from eqs 18 and 19, we obtain

$$1/\alpha = 1/K + (L/K)\eta \tag{21}$$

where

$$K = [(B - A) + (a_0 - b_0) + (b_0A - a_0B)]/(1 - B) \tag{22}$$

$$L = [(1 - \cot^2\theta) - A + (1 + \cot^2\theta)B]/[3(1 - \cot^2\theta)(1 - B)] \tag{23}$$

$$\alpha = (e^2q_{zz}Q)/(e^2q_0Q) \tag{24}$$

This predicts a linear relationship between $1/\alpha$, the reciprocal of the reduced quadrupole coupling constant, and the asymmetry parameter η, for the series of imidazole derivatives examined. The slope of the line is $1/K$ and the intercept is L/K.

Figure 7 is a plot of $1/(e^2qQ)$ vs η for various substituted imidazoles and for copper proteins (quadrupole coupling constants and asymmetry parameters are listed in Table II for model compounds and in Table III for copper proteins). A straight line fit to the model compound data was obtained by a first-order regression. The data points for the model compounds gather at three regions of the line, corresponding to the three groups of compounds listed in Table II. Deviation from the line, such as **10**, is attributed to differences in geometry and in electron occupancy of the two N–C ring sp^2 orbitals caused by 5-Cl substitution, while deviation of **5** and **6** from the line is attributed to the imprecise measurement of frequency due to the poor resolution of the first two quadrupolar lines in the ESEEM spectrum.

The protein data, also plotted in Figure 7, fit the line well. This suggests that the assumptions made concerning the CNC angle and the linear inductive relationship concerning orbital occupancy for the model compounds are also valid for the proteins. Therefore, we are able to relate the electron orbital occupancy for the remote nitrogen of the histidine imidazole ligand in a copper protein to that of the reference compound by eqs 13 and 14, as we have done for the various substituted imidazoles.

Values of 0.401 and 0.294 are obtained as the intercept and slope, respectively, in Figure 7, which can be used to determine L (eq 21). From eq 23 and the value of 2θ, 107.2°, obtained from

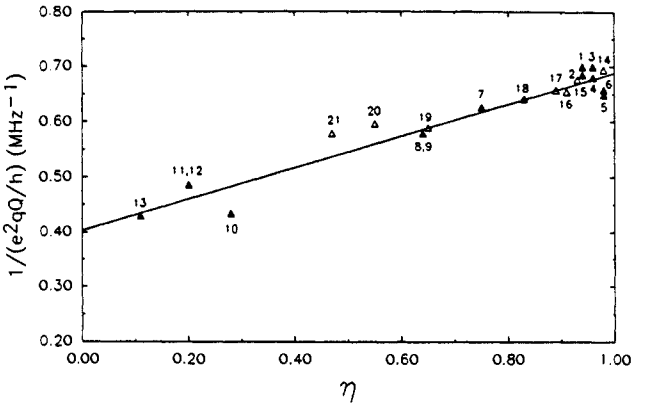

Figure 7. A plot of the reciprocal of the quadrupole coupling constant e^2qQ vs the asymmetry parameter η for Cu(II)–dien-substituted imidazole model compounds and copper proteins. The numbers refer to compounds in Tables II and III: filled triangles, Cu(II)–dien-substituted imidazole model compounds and open triangles, Cu(II) proteins.

a single-crystal X-ray study,[32] we obtain the linear relationship between A and B as

$$A = 1.275B + 0.275 \tag{25}$$

The relationship between A and B is also expressed in eq 22. However, this equation contains two unknowns, a_0 and b_0, which cannot be derived from e^2qQ and η for the reference compound, 1,2-dimethylimidazole, without expressing them in terms of another unknown, c_0. Therefore, this relationship cannot be used to determine A and B.

Considering the constraints imposed by the physical meaning of A and B, that is $0 < A + 2B < 1$, and the linear relationship of eq 22, A and B may vary between 0.275 and 0.557 and 0 and 0.221, respectively. By using the same argument as Ashby et al.[27,30] for the imino nitrogen of metal-bound imidazole as well as for metal-bound pyridine, that is by choosing the midrange values for A and B, we obtain 0.409 and 0.105, respectively, for the remote nitrogen of imidazole. Therefore, $A + 2B = 0.620$; that is 62.0% of the change of electron occupancy in the N–H sp^2 orbital can be compensated for by the inductive electron flow from other orbitals. From a comparison between the calculated values of A and B that we obtain for the remote nitrogen of imidazole, with the published values, 0.400 and 0.110, for the imino nitrogen of metal-coordinated imidazole,[27] we suggest that the inductive responses of the nitrogen ring N–C sp^2 orbitals and the $p\pi$ orbital to the external N–H sp^2 orbital are very similar for both amino and imino nitrogen.

Model Compounds and Change of Electron Orbital Occupancy. From a knowledge of A and B, we may plot three principal values of the quadrupole coupling tensors as a function of $c - c_0$ and compare them with those calculated from experimental values of

(32) Potenza, M. N.; Potenza, J. A.; Schugar, H. J. *Acta Crystallogr.* **1988**, *C44*, 1201–1204.

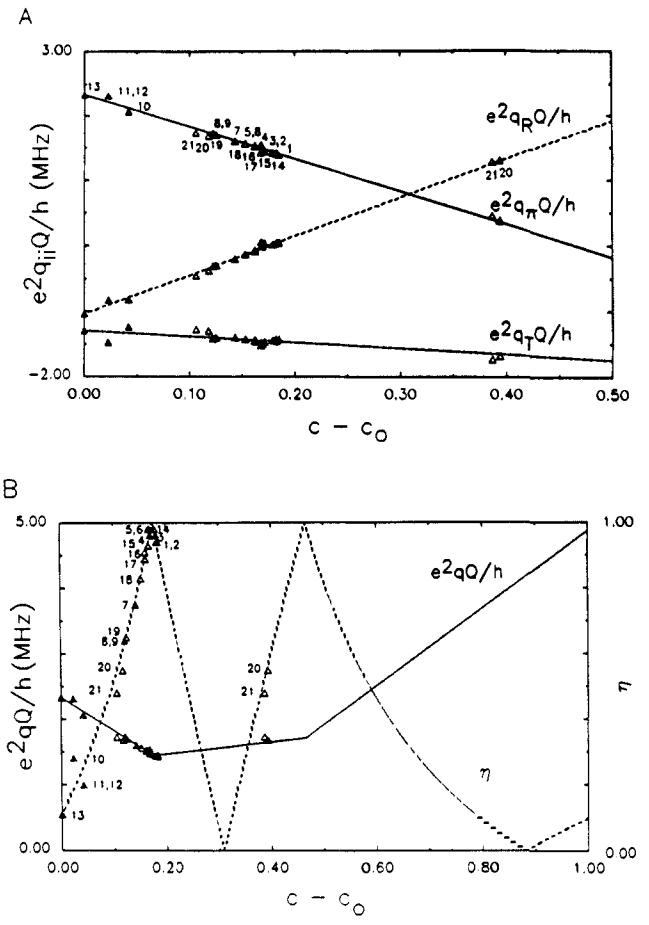

Figure 8. (A) Plot of $e^2q_{ii}Q/h$ vs N–H or N–C sp^2 orbital population change, $c - c_0$, for model compounds and copper proteins: solid line, $e^2q_\pi Q/h$; dashed line, e^2q_RQ/h; dashed dot line, e^2q_TQ/h. (B) Plot of e^2qQ/h and η vs N–H or N–C sp^2 orbital population change, $c - c_0$, for Cu(II)–dien-substituted imidazole model compounds and copper proteins: solid line, e^2qQ/h; dashed line, η. The regions are represented as follows: region I, $0 < c - c_0 < 0.172$, where η has the first positive slope; region II, $0.172 < c - c_0 < 0.304$, where η has the first negative slope; and region III, $0.304 < c - c_0 < 0.462$, where η has the second positive slope. The symbols are the following: filled triangles, model compounds; open triangles, copper proteins. The number for each complex and protein is referred to in Tables II and III.

e^2qQ and η for model compounds and copper proteins (shown in Figure 8A). The value of $c - c_0$ that gives the best correspondence between experimental and theoretical values for each compound can be obtained by minimizing the quantity

$$\delta = (\delta_x^2 + \delta_y^2 + \delta_z^2)^{1/2} \qquad (26)$$

where $\delta_i (i = x, y, z)$ is the difference between the experimental and calculated ith principal value of the quadrupole coupling tensor.[30] By assigning the largest principal values of **efg** as q_{zz}, we can also plot e^2qQ/h and η for each model compound and copper protein as a function of $c - c_0$ according to eqs 18 and 19. Figure 8B shows such a plot and also the experimental values of e^2qQ/h and η at $c - c_0$ obtained by minimization of δ. The values of $c - c_0$ are collected in Table II.

In Figure 8B, the quadrupole parameters for the model compounds are shown to fall in two regions. In region I, where $|q_\pi| > |q_T| > |q_R|$ and $c - c_0 < 0.176$, the largest **efg** axis, q_{zz}, is normal to the ring plane, and the second largest **efg** axis is in the ring plane and perpendicular to the N–H or N–R bond. In this region, the decrease of e^2qQ and increase of η corresponds to an increase of $c - c_0$. In region II, where $|q_T| > |q_\pi| > |q_R|$, $0.176 < c - c_0 < 0.307$, a switch of the largest **efg** axis from perpendicular to the ring plane to in-plane and perpendicular to the N–H bond has taken place. In this region, the increase of e^2qQ and decrease of η corresponds to an increase of $c - c_0$. In region III, where $|q_T| > |q_R| > |q_\pi|$ and $0.307 < c - c_0 < 0.465$, the largest **efg** axis is in-plane and perpendicular to the N–H bond, the same as in region II. However, the second largest **efg** axis switches from perpendicular to the ring plane to in-plane and along the N–H bond.

Most model compounds fit in region I of Figure 8B. Three N-alkylated model compounds, **10**, **11**, and **12**, with a large e^2qQ and a small η, have small values of $c - c_0$. This indicates that the value of c for each of them is not very different from that of the reference compound, 1,2-dimethylimidazole. Upon N-dealkylation, as for **7**, **8**, and **9** in group 2, the values of $c - c_0$ increase to about $^2/_3$ of the maximal value observed for the model compounds (Table II). The remainder of the model compounds are in group 1 and occupy a region in Figure 8B bordering regions I and II. Their values of $c - c_0$ are the largest obtained for all the model compounds studies.

The placement of imidazole in Figure 8B is close to the confluence of regions I and II. Because both e^2qQ and η reflect at the border of region I and region II, there is some ambiguity at which side to place imidazole. The smallest δ (eq 26), 0.037, can be obtained by fitting imidazole in region II. A larger value of δ, 0.076, is obtained by fitting imidazole in region I. Even though δ is twice as large in the latter case, the difference between the theoretically predicted values of e^2qQ and η and those determined experimentally are still within experimental error.[33] But no matter which region it is placed, values of $c - c_0$ for imidazole and other group 1 compounds are larger than those for 2-methylimidazole and other group 2 compounds and which, in turn, are larger than those for N-alkylated group 3 compounds. The increase of η, then, is due to the increase of the electron occupancy in the N–H or N–R sp^2 orbital.

Hydrogen Bonding. An infrared study of solid $Zn(II)(imid)_2X_2$ (X = Cl, Br, I)[27] showed that the N–H stretching frequency of imidazole increases with the size of the halide. The complex containing chloride, the smallest halide in the series, then has the lowest N–H stretching frequency. Since chloride is better able to form intramolecular hydrogen bonds than either bromide or iodide, the N–H bond in the chloride complex must be weakened by strong hydrogen bond formation. Therefore, the magnitude of the N–H stretching frequency is inversely related to the strength of the hydrogen bond that is formed. A parallel NQR study[27] carried out on the same compounds showed that the electron occupancy of the imidazole N–H sp^2 orbital increases when its stretching frequency decreases. For the complex with chloride, which forms the strongest hydrogen bond and where the complex has the smallest N–H stretching frequency, the N–H electron occupancy c is larger than that for the bromide complex, which in turn is larger than that for the iodide complex. Thus, the magnitude of c can be taken as an indicator of N–H bond polarizability and the extent of hydrogen bonding.

In another study, it was shown that the NQI parameters for imidazole in the gas phase ($e^2qQ = 2.54$, $\eta = 0.18$)[34] are quite different from those in the solid ($e^2qQ = 1.42$, $\eta = 0.99$).[25] This difference is much larger than observed for pyridine ($e^2qQ = 4.87$, $\eta = 0.42$ gas;[35] $e^2qQ = 4.58$, $\eta = 0.40$ solid[30]), and for this reason cannot be completely attributed to phase effects. In both gaseous and solid phases, pyridine nitrogen does not form hydrogen bonds. For solid imidazole, on the other hand, the amino nitrogen is capable of forming a hydrogen bond with another imidazole molecule, and this does not occur in the gas phase. Therefore, the differences observed for imidazole between gas and solid phases are largely attributed to hydrogen bond formation in the solid.

(33) The errors in the spectral simulation are variable for different groups of model compounds. For group 1 model compounds, the poor resolution of the two low-frequency lines reduces the accuracy of the simulation. Errors of 0.04 MHz and 0.05 for e^2qQ and η must be introduced in simulations for group 1 model compounds to observe a significant change. Errors for group 2 model compounds are 0.02 MHz and 0.03, since the three NQI lines are well resolved. Errors for group 3 are 0.04 MHz and 0.05 due to the lack of resolution of the lowest line because of instrumental limitions.

(34) Blackman, G. L.; Brown, R. D.; Burden, F. R.; Elsum, I. R. *J. Mol. Spectrosc.* **1976**, *60*, 63–70.

(35) Sørensen, G. O.; Mahler, L.; Rastrup-Andersen, N. *J. Mol. Struct.* **1974**, *20*, 119–126.

In our study of imidazole and *N*-alkylimidazole coordinated to Cu(II)–dien, it was shown that $c - c_0$ for the former is much larger than for the latter. Since the NQI parameters for Cu(II)–dien–*N*-benzylimidazole ($e^2qQ = 2.06$, $\eta = 0.20$, Table II) are comparable to those for solid *N*-benzylimidazole ($e^2qQ = 2.20$, $\eta = 0.23$)[27] as well as for imidazole in the gas phase, this suggests that the electron occupancy at the external N–C sp^2 orbital of solid *N*-benzylimidazole, either uncoordinated or coordinated to Cu(II)–dien is similar to the electron occupancy at the remote N–H sp^2 orbital of imidazole in the gas phase. The values of $c - c_0$ in all three instances are therefore much lower than for imidazole coordinated to Cu(II)–dien or for imidazole in the solid state. Since no hydrogen bond can be formed in N-alkylated derivatives, the increase in $c - c_0$ for Cu(II)–dien-coordinated imidazole and solid-state imidazole must primarily stem from hydrogen bond formation with imidazole.

Solvent Effects. Exchange of solvent protons with deuterons changes the ESEEM spectra of Cu(II)–dien–imidazole and Cu(II)–dien–2-methylimidazole where the remote nitrogen is protonated. As shown in Figure 9A, the two poorly resolved low-frequency NQI lines of Cu(II)–dien–imidazole in H_2O (Figure 1B) are now resolved in D_2O to give two well-separated lines. This indicates that D_2O lowers the asymmetry parameter η, which correlates with a decrease of the electron occupancy $c - c_0$ in the N–H sp^2 orbital. In contrast, the ESEEM spectrum of Cu(II)–dien–1-methylimidazole, where the remote nitrogen is alkylated remains unchanged in D_2O. Because the CW EPR spectra of all the complexes remain the same in H_2O and D_2O, there is no change of geometry around the Cu(II) due to solvent effects. It is the replacement of N–H by N–D that results in the changes of η observed in ESEEM spectra of N-dealkylated Cu(II)–dien-substituted imidazole complexes. Therefore, the replacement of N–H by N–D reduces the electron occupancy of the external sp^2 orbital at the remote nitrogen and weakens the hydrogen bond between this nitrogen with solvent water or excess imidazole.

Deuterium isotope effects in hydrogen bonding have been observed in many O–H···O systems. For a strong O–H···O hydrogen bond, it has been shown that the replacement of H by D increases the O···O distance.[36] This indicates the weakening of the hydrogen bond, which is consistent with the isotope effect we observe for the remote nitrogen of Cu(II)–dien–imidazole in D_2O.

Formate also changes the ESEEM spectra of Cu(II)–dien–imidazole and Cu(II)–dien–2-methylimidazole. This change too is attributed to a change of hydrogen bonding. In contrast to the effect of D_2O, formate moves the two low-frequency lines in the ESEEM spectra closer to one another. (Compare the spectra of Cu(II)–dien–2-methylimidazole in the presence of formate (Figure 9B) and in its absence (Figure 1D).) This indicates that formate increases the asymmetry parameter η and changes the **efg** at the remote nitrogen of coordinated imidazole.

The change of **efg** can arise not only from a change of electron orbital occupancy through hydrogen bonding but also from the introduction of charge. The carboxyl group of formate, which has the potential to form a hydrogen bond with the remote nitrogen of imidazole, has a negative charge not present in water or excess imidazole. One would think that this charge could alter the **efg**. The ESEEM spectrum of Cu(II)–dien–1-methylimidazole is not altered by formate, and the **efg** at the remote nitrogen remains the same. Any possible change of the **efg** generated by a negative charge of formate is therefore undetectable. The changes of **efg** observed in Cu(II)–dien–imidazole and Cu(II)–dien–2-methylimidazole do not arise from an increase of negative charge introduced by formate but rather from a change of the electron occupancy of the nitrogen orbital. Therefore, the increase of η by formate is attributed to an increase of the electron occupancy $c - c_0$, which indicates the strengthening of the hydrogen bond at the imidazole remote nitrogen.

Figure 9C shows that Cu–dien–imidazole studied in D_2O and formate has the same spectrum as it has in H_2O. This suggests that the effects from deuterium and formate cancel each other, which further confirms that deuterium weakens the hydrogen bond while formate strengthens it.

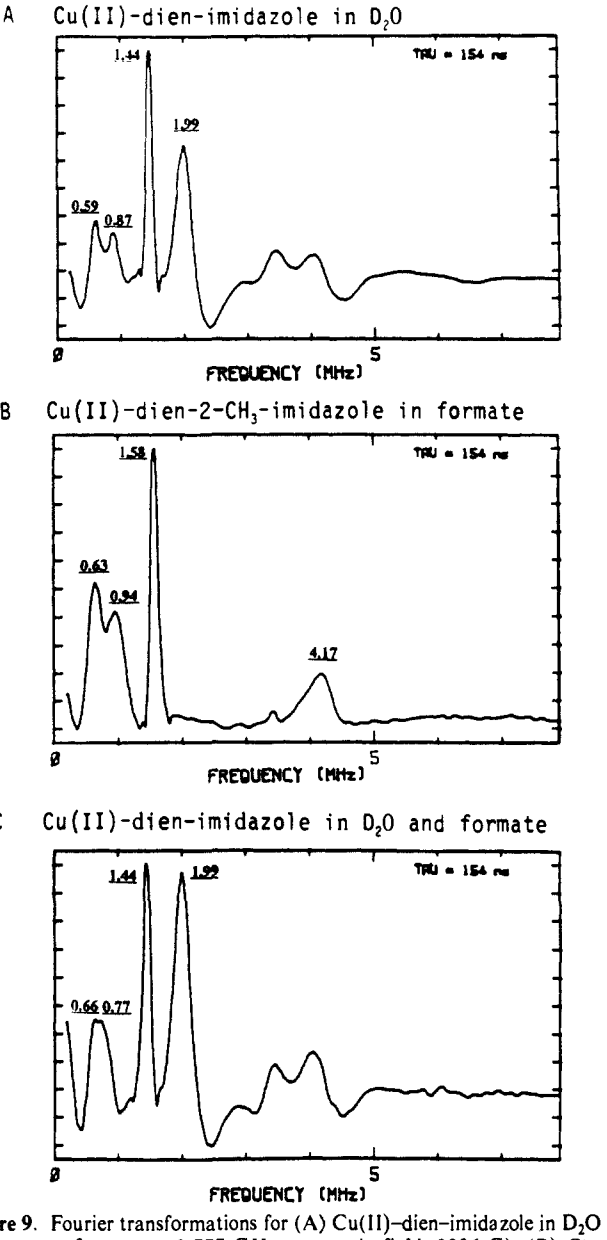

Figure 9. Fourier transformations for (A) Cu(II)–dien–imidazole in D_2O (microwave frequency, 8.777 GHz; magnetic field, 3036 G), (B) Cu(II)–dien–2-methylimidazole in the presence of sodium formate (~6 M) (microwave frequency, 8.795 GHz; magnetic field, 3036 GHz), and (C) Cu(II)–dien–imidazole in D_2O and formate (microwave frequency, 8.813; magnetic field, 3036 G). The frequency component at 1.99 MHz in (A) and (C) arises from weakly coupled ^2H.

Bond Polarization and Binding Affinity. When imidazole binds to Cu(II)–dien, the imino nitrogen donates its lone pair electrons to Cu(II) and bears a partial positive charge (I). This charge can delocalize to the aromatic π system (II). In the presence of a nucleophile, the charge can then delocalize further onto the amino or remote nitrogen through the formation of a hydrogen bond (III), whose presence polarizes the N–H bond. If, however, the remote nitrogen of imidazole is alkylated, or there is no nucleophile near the remote nitrogen, the less polarized N–C bond (due to the higher electronegativity of C) or N–H (due to the lack of hydrogen bonding) prevents the delocalization of the positive charge and leads to a lowered affinity of metal for ligand (Table I). Therefore, the reduction of polarization at the N–H bond of imidazole would lower the affinity of imidazole for Cu(II)–dien, and conversely, the reduction of the affinity of imidazole for Cu(II)–dien would reduce the polarization of the N–H bond.

2-Methylimidazole is more basic than imidazole (Table I), and this would suggest that the former should bind more strongly to a metal ion. However, optical titrations show that imidazole rather than 2-methylimidazole has a greater affinity for Cu(II)–dien.

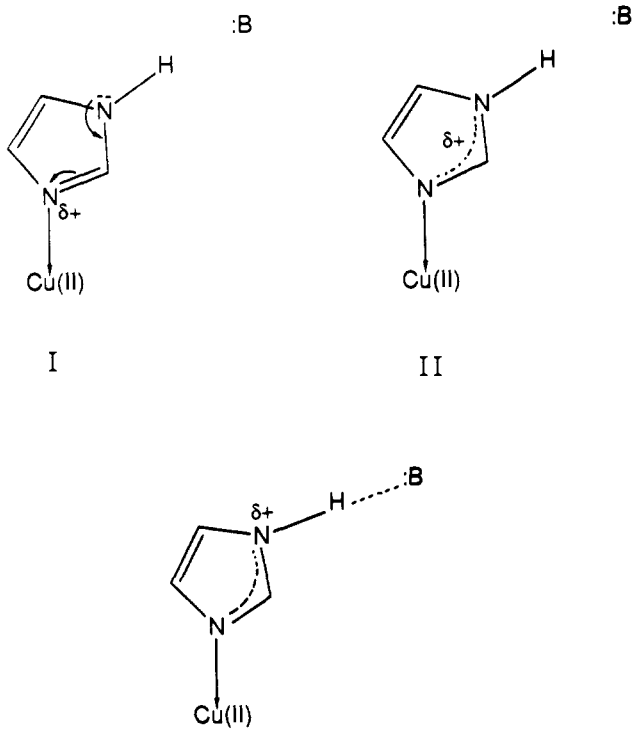

This is believed to be due to the presence of a bulky group adjacent to the imino nitrogen of 2-methylimidazole, which sterically hinders its binding to Cu(II)-dien. As a consequence of weaker binding, less positive charge is delocalized from Cu(II) to the imidazole ring, leaving the N–H bond at the remote nitrogen less polarized. This is reflected in the $c - c_0$ value for 2-methylimidazole which is only $^2/_3$ of that for imidazole. Therefore, even though the remote nitrogen of 2-methylimidazole would readily form hydrogen bonds with solvent or other ligand molecule, the reduced affinity of 2-methylimidazole, probably due to steric hinderance, would result in the formation of a weaker hydrogen bond, as compared to imidazole.

This view is supported by a binding study of imidazole and its *N*-methyl and 2-methyl derivatives to Fe(III)–tetraphenylporphyrin. Walker et al.[13] showed that the removal of hydrogen-bonding capabilities of imidazole by N-alkylation markedly reduces ligand affinity. Placing a bulky substituent at the 2-position has a comparable effect. This suggests that the extent of polarization of the N–H bond of imidazole in the absence of hydrogen bonding is equivalent to the placement of a bulky group at the 2-position.

Geometric Effects. It has been shown that for Zn(II)-coordinated imidazole complexes in the solid state, the variation of c with change of site symmetry (octahedral versus tetrahedral) is small, with differences as little as 0.004. In contrast, the variation of c with change of anion leading to alteration in intramolecular hydrogen bonding ($Zn(Im)_2Cl_2$ versus $Zn(Im)_2Br_2$), may be considerable, as much as 0.036.[27]

In Cu(II) proteins, which may be prone to geometric alteration around the metal center, it is not likely that site symmetry differences affect N–H bond polarizability to the same degree as hydrogen bond formation. Therefore, even though a geometric change may take place around a Cu(II) center, it is likely the strength of the hydrogen bond at the remote nitrogen of the histidine side chain that changes c. By fitting e^2qQ and η for copper proteins, we may predict the strength of a putative hydrogen bond from a value of $c - c_0$.

Copper Proteins. Protein data fall into three regions of Figure 8B. On the basis of the magnitude of $c - c_0$ (Table III), it is suggested that **16**, **17**, and **18** form strong hydrogen bonds at the remote nitrogen of a coordinated histidine side chain, either with a protein moiety or a solvent molecule. Protein **19** falls into region I indicating that it has a weak hydrogen bond at the remote nitrogen. For proteins **20** and **21**, data fall either into region I or region III, the latter containing no data for any imidazole model thus far examined. The ambiguity in placement arises from the fact that e^2qQ varies little in region II and III, with large variation in $c - c_0$. Were the data for these proteins to fall in region I, this would suggest that Cu(II)-coordinated histidine imidazole would not form a hydrogen bond or would form a very weak hydrogen bond. Were the data to fall in region III, we would be required to refine our analysis further.

In order to understand the physical meaning of region III, we would require the absolute value of electron orbital occupancy, c. Because no reasonable assumption can be made for a value of c_0 to obtain a_0 and b_0 (eqs 10–12) for the amino nitrogen of 1,2-dimethylimidazole and the inductive response among different orbitals of both nitrogens are the same, we use the imino nitrogen of metal-free *N*-benzylimidazole, the same reference compound as in refs 27 and 37. Here, the electron occupancy of the external sp^2 orbital of the imino nitrogen, c_0 (σ in ref 27), is assumed to be 2, because the alkylated amino nitrogen of *N*-benzylimidazole cannot form a hydrogen bond so as to perturb the electron charge distribution of the lone pair orbital of the imino nitrogen. The values of a_0 and b_0 are then determined as 1.026 and 1.018. With the use of the same values of A, B, and θ as before, we obtain the absolute value of electron orbital occupancy c for each model compound and copper protein by the minimization scheme noted above (eq 26). The change of the electron occupancy at the external sp^2 orbital from that of 1,2-dimethylimidazole for all the 21 model compounds and proteins are consistent with the values of $c - c_0$ obtained before, within 0.001. Further, we obtain a value of c, 1.147, for our first reference compound, 1,2-dimethylimidazole, and 1.541 and 1.534 for proteins **20** and **21**.

There are two ways to increase the electron occupancy of the external sp^2 orbital of the remote nitrogen. One is through formation of a hydrogen bond and the other through deprotonation. If the remote nitrogen is deprotonated, then c should be very close to 2. Because the values of c for proteins **20** and **21** are considerably smaller, their placement in region III cannot be substantiated by the deprotonation mechanism. NQR[38] and neutron diffraction studies[39] of crystalline imidazolium hydrogen maleate showed that the three principal values of the **efg** tensor are arranged as $|q_T| > |q_\pi| > |q_R|$, placing it in region II (Figure 8B). In this compound, N–H $\approx$ 1.07 Å, N···O $\approx$ 2.64 Å, and the N–H···O angle is near 171°. As the N–H···O bond is nearly linear and the N···O distance is shorter than the combined van der Waals radius for N and O, the hydrogen bond formed is very strong. Since the formation of such a strong hydrogen bond still cannot polarize the N–H bond to the extent that switches the **efg** axis to place the compound in region III, there is no reasonable mechanism for the placement of proteins **20** and **21** in region III, and we conclude that they should also be in region I like other copper proteins. We suggest that the Cu(II)-coordinated histidine side chains of these two proteins are in a hydrophobic environment or form weak hydrogen bonds.

Summary. In conclusion, we relate the NQI parameters for Cu(II)-coordinated imidazole obtained by ESEEM measurements to the electron orbital occupancy of the remote nitrogen, which can be taken as indicators of the bond strength of the remote N–H bond of a coordinated histidine side chain in proteins. Since the strength of the N–H bond is partly determined by the strength of the hydrogen bond formed with solvent or protein side-chain

(36) Pimentel, G. C.; McClellan, A. L. *The Hydrogen Bond*; W. H. Freeman and Company: San Francisco and London, 1960; pp 225–296.
(37) Ashby, et al.[27c] used the same reference compound and the same parameters to fit the data of the imino nitrogen as well as the amino or the remote nitrogen. Their fitting of e^2qQ and η for the amino nitrogen was not as good as for the imino nitrogen, but they did obtain a reasonable fit for three principal values of the quadrupolar coupling tensor for the former.
(38) Palmer, M. H. *Chem. Phys.* **1987**, *115*, 207–218.
(39) (a) Hsu, B.; Schlemper, E. O. *Acta Crystallogr.* **1980**, *B36*, 3017–3023. (b) Hussain, M. S.; Schlemper, E. O.; Fair, C. K. *Acta Crystallogr.* **1980**, *B36*, 1104–1108.

nucleophiles, we can predicate the strength of the hydrogen bond from the electron orbital occupancy of the remote nitrogen. For those proteins studied by ESEEM, we suggest that the histidine ligands of Cu(II) sites in stellacyanin and dopamine β-hydroxylase form strong hydrogen bonds, while for galactose oxidase, amine oxidase, and phenylalanine hydroxylase a much weaker or no hydrogen bond is present.

Acknowledgment. This work was supported by U.S.P.H.S. Grants GM 40168 and RR 02583 from the National Institutes of Health. We thank Richard S. Magliozzo, Michael J. Colaneri, and Jeffery B. Cornelius for helpful discussions.

Reaction of Anions with Activated Olefins in the Gas Phase. A Flowing Afterglow–Selected Ion Flow Tube Study

Claude F. Bernasconi,*,† Michael W. Stronach,† Charles H. DePuy,‡ and Scott Gronert‡

Contribution from the Thimann Laboratories of the University of California, Santa Cruz, California 95064, and the Department of Chemistry and Biochemistry of the University of Colorado, Boulder, Colorado 80309-0215. *Received February 20, 1990. Revised Manuscript Received May 9, 1990*

Abstract: Reactions of anions with acrylonitrile, acrolein, methyl vinyl ketone, and methyl acrylate at room temperature under SIFT conditions are described. Stabilized carbanions such as benzyl anion, cyanomethyl anion, cyclohexadienide, acetone enolate, and nitromethyl anion add to activated carbon–carbon double bonds in a process that is competitive with other modes of reaction. With acrylonitrile and methyl acrylate, addition is in a 1,4 or Michael fashion, while with acrolein and methyl vinyl ketone, 1,2 addition competes with 1,4 addition. Hydroxide, methoxide, fluoride, and cyanide do not add to activated olefins by either mode (see Tables I–IV). A mechanism is proposed for hydride transfer from cyclohexadienide to activated olefins.

Reaction of anions with neutral organic molecules in the gas phase gives rise to a wide variety of products, including those that can be ascribed to the processes of proton transfer,[1] elimination,[2] substitution,[3] and attack at the carbon of carbonyl groups.[4] Using activated olefins such as acrylonitrile (**1**), acrolein (**2**), methyl vinyl ketone (**3**), and methyl acrylate (**4**) presents the opportunity for

$CH_2{=}CHCN$ (**1**) $CH_2{=}CHCHO$ (**2**) $CH_2{=}CHCOCH_3$ (**3**) $CH_2{=}CHCOOCH_3$ (**4**)

1,4 addition to carbon–carbon double bonds. A reaction of this type is of interest because it represents the gas-phase equivalent of a 1,4 or Michael addition. The work described shows that certain anions add to activated double bonds in the gas phase in a process that is competitive with other modes of reaction.

The tandem flowing afterglow–selected ion flow tube technique[5] was used to examine the reactivity pattern of **1–4** toward a range of anionic nucleophiles including the following: hydroxide, methoxide, benzyl anion, cyanomethyl anion, cyclohexadienide, fluoride, acetone enolate, nitromethyl anion, and cyanide. In many instances, peaks were prominent in the product mass spectrum indicating combination of olefin and anion to make a species that might be a cluster or a 1,4 or 1,2 adduct (eqs 1–3). Identifying

$$Nuc^- + CH_2{=}CHCHO \rightarrow [Nuc{\cdot}CH_2{=}CHCHO]^- \quad \text{cluster} \quad (1)$$

$$Nuc^- + CH_2{=}CHCHO \rightarrow Nuc\text{-}CH_2C^-HCHO \quad \text{1,4 adduct} \quad (2)$$

$$Nuc^- + CH_2{=}CHCHO \longrightarrow CH_2{=}\underset{\displaystyle Nuc}{\overset{\displaystyle O^-}{\underset{|}{\overset{|}{C}}}}H \quad \text{1,2 adduct} \quad (3)$$

the structure of these adducts is an interesting challenge, since mass spectrometry alone cannot give the structure of an observed ion. There were also peaks in the mass spectrum for deprotonation, the elimination of cyanide from acrylonitrile, and the cleavage of acrylate from methyl acrylate, along with other side reactions discussed under Results.

The main goal of these experiments was to look for addition of anions to carbon–carbon double bonds. Finding an addition peak in the product mass spectrum with the correct m/z ratio was the first step. Reaction with various deuterated reagents or butyl nitrite was then used to probe the structure of the adducts and determine if they were clusters, 1,4 adducts or 1,2 adducts.

Each type of product has characteristic reactions that allow the structure of the anion to be probed. For example, since clusters are held together by ion–dipole forces, interacting a cluster with a reagent such as water, acetone, or the perdeuterated neutral

† University of California.
‡ University of Colorado.

(1) (a) Pellerite, M. J.; Brauman, J. I. In *Comprehensive Carbanion Chemistry—Part A, Structure and Reactivity*; Buncel, E., Durst, T., Eds.; Elsevier: Amsterdam, 1980. (b) Moylan, C. R.; Brauman, J. I. *Annu. Rev. Phys. Chem.* **1983**, *34*, 187–215.

(2) (a) Bartmess, J. E.; Hays, R. L.; Khatri, H. N.; Misra, R. J.; Wilson, S. R. *J. Am. Chem. Soc.* **1981**, *103*, 4746. (b) DePuy, C. H.; Bierbaum, V. M. *J. Am. Chem. Soc.* **1981**, *103*, 5034–5038. (c) DePuy, C. H.; Beedle, E. C.; Bierbaum, V. M. *J. Am. Chem. Soc.* **1982**, *104*, 6483. (d) Bierbaum, V. M.; Filley, J.; DePuy, C. H.; Jarrold, M. F.; Bowers, M. T. *J. Am. Chem. Soc.* **1985**, *107*, 2818–2820. (e) Jones, M. E.; Ellison, G. B. *J. Am. Chem. Soc.* **1989**, *111*, 1645–1654.

(3) (a) Tanaka, K.; MacKay, G. I.; Payzant, J. D.; Bohme, D. K. *Can. J. Chem.* **1976**, *54*, 1643–1659. (b) Olmstead, W. N.; Brauman, J. I. *J. Am. Chem. Soc.* **1977**, *99*, 4219–4228. (c) Pellerite, J.; Brauman, J. I. *J. Am. Chem. Soc.* **1983**, *105*, 2672–2680. (d) Van Doren, J. M.; DePuy, C. H.; Bierbaum, V. M. *J. Phys. Chem.* **1989**, *93*, 1130–1134. (e) Lum, R. C.; Grabowski, J. J. *J. Am. Chem. Soc.* **1988**, *110*, 8568–8570.

(4) (a) Asubiojo, O. I.; Brauman, J. I. *J. Am. Chem. Soc.* **1979**, *101*, 3715–3724. (b) Bartmess, J. E.; Hays, R. L.; Caldwell, G. *J. Am. Chem. Soc.* **1981**, *103*, 1338–1344. (c) DePuy, C. H.; Grabowski, J. J.; Bierbaum, V. M.; Ingemann, S.; Nibbering, N. M. M. *J. Am. Chem. Soc.* **1985**, *107*, 1093–1098.

(5) (a) Adams, N. G.; Smith, D. *Int. J. Mass Spectrom. Ion Phys.* **1976**, *21*, 349–359. (b) Bierbaum, V. M.; DePuy, C. H.; Shapiro, R. H.; Stewart, J. H. *J. Am. Chem. Soc.* **1976**, *98*, 4229. (c) Smith, D.; Adams, N. G. In *Gas Phase Ion Chemistry*, Bowers, M. T., Ed.; Academic Press: New York, 1979; Vol. 1, pp 1–44. (d) DePuy, C. H.; Bierbaum, V. M. *Acc. Chem. Res.* **1981**, *14*, 146–153. (e) For a recent review of flow reactor techniques, see: Graul, S. T.; Squires, R. R. *Mass Spectrom. Rev.* **1988**, *7*, 263–358.

0002-7863/90/1512-9044$02.50/0